

## Electronic Supplementary Information

### **Iron(III) carboxylate/aminoalcohol coordination clusters with propeller-shaped Fe<sub>8</sub> cores: approaching reasonable exchange energies**

Olga Botezat,<sup>a,b</sup> Jan van Leusen,<sup>b</sup> Victor Ch. Kravtsov,<sup>a</sup> Arkady Ellern,<sup>c</sup> Paul Kögerler,<sup>b,\*</sup> and Svetlana G. Baca<sup>a,\*</sup>

*<sup>a</sup>Institute of Applied Physics, Academy of Science of Moldova, Academiei 5, MD2028 Chisinau, Moldova*

*<sup>b</sup>Institute of Inorganic Chemistry, RWTH Aachen University, Landloweg 1, 52074 Aachen, Germany*

*<sup>c</sup>Department of Chemistry, Iowa State University, Ames, USA*

#### **Corresponding Authors**

\*E-mail: paul.koegerler@ac.rwth-aachen.de (P.K.), sbaca\_md@yahoo.com (S.G.B).

Tel: +49-241-80-93642 (P.K.), +373-22-738154 (S.G.B.).

Fax: +39-241-80-92642 (P.K.), +373-22-738149 (S.G.B.).

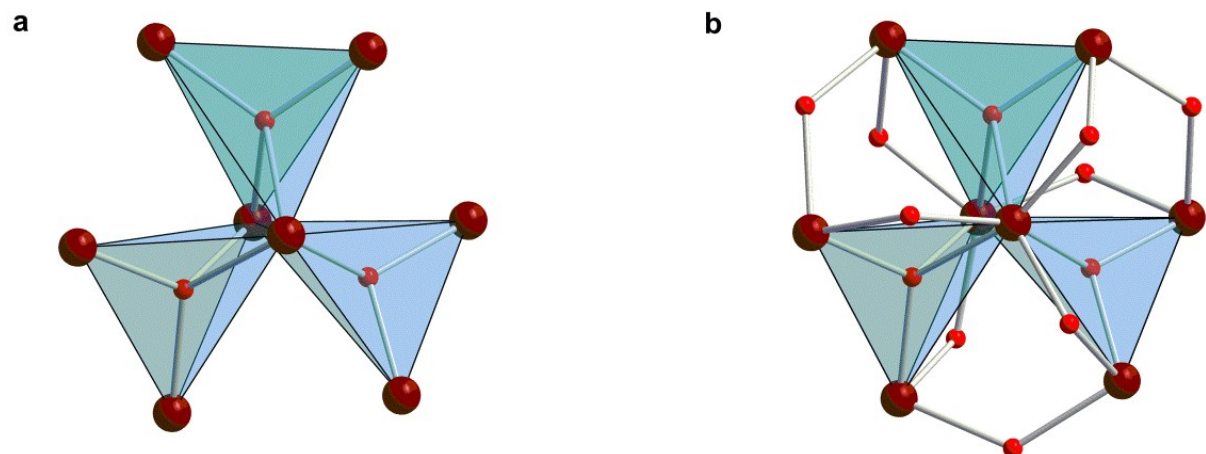


**Figure S1.** The propeller-shaped metal oxide core in compounds **1–4**: a view of (a) the  $\{\text{Fe}_8\text{O}_3\}$  core with three  $\mu_4$ -oxygen atoms and (b) the  $\{\text{Fe}_8\text{O}_{12}\}$  core with three  $\mu_4$ -oxygen atoms and nine bridging alkoxide oxygen atoms of the triethanolamine ligands in **1–3** or three  $\mu_4$ -oxygen atoms, six bridging alkoxide oxygen atoms of the N-methyldiethanolamine and three oxygen atoms of methoxy groups in **4**. Color scheme: Fe: brown spheres; O: red spheres.

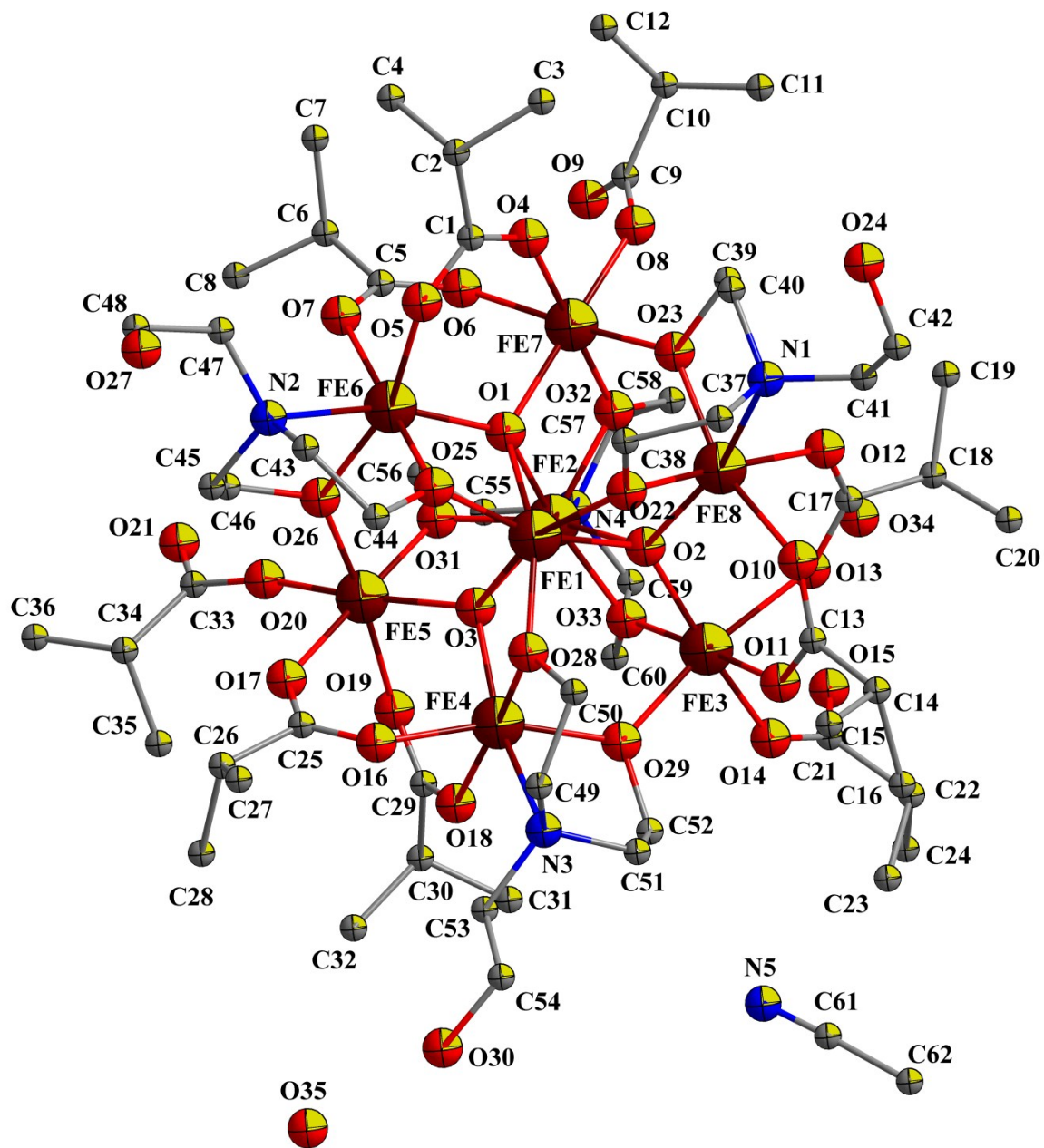


**Figure S2.** Asymmetric unit in the solid-state structure of  $[\text{Fe}_8\text{O}_3(\text{O}_2\text{CCHMe}_2)_9(\text{tea})(\text{teaH})_3] \cdot \text{MeCN} \cdot 2(\text{H}_2\text{O})$  (**1**) with atom numbering scheme. Hydrogen atoms and disorder C atoms are omitted for clarity.

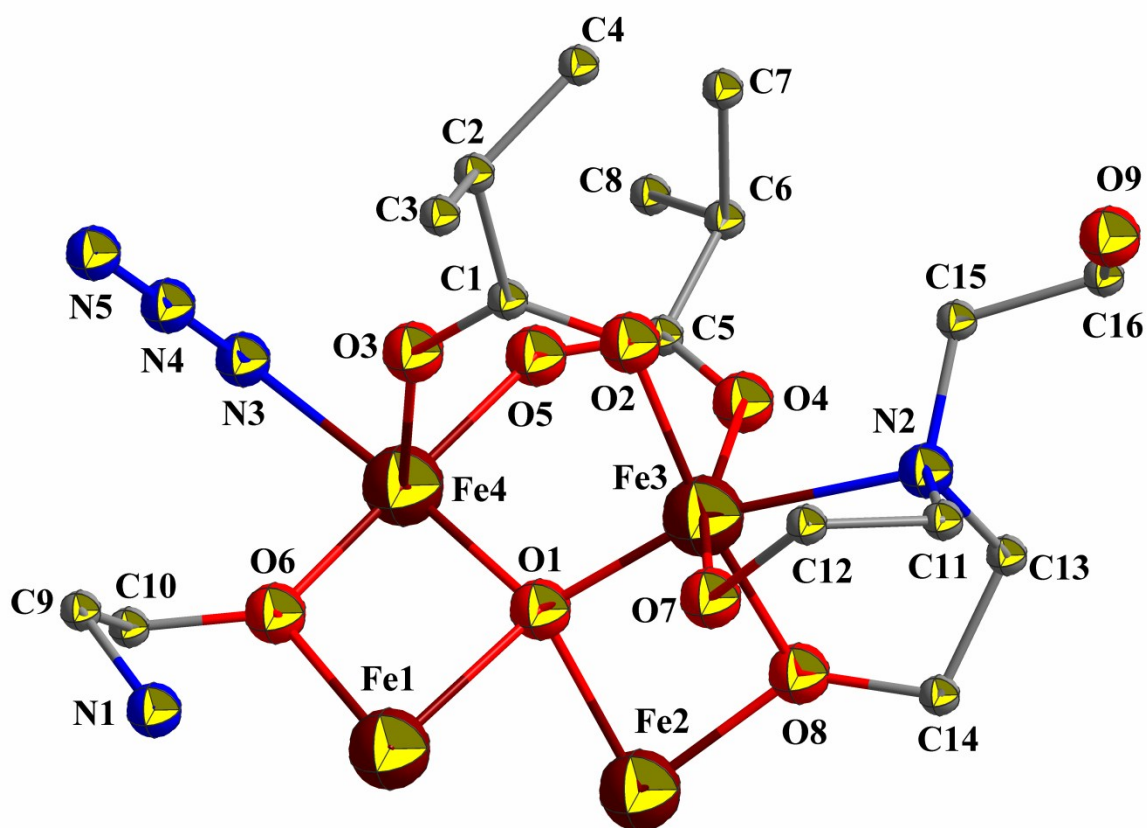


**Figure S3.** Asymmetric unit in the solid-state structure of  $[\text{Fe}_8\text{O}_2(\text{O}_2\text{CCHMe}_2)_6(\text{N}_3)_3(\text{tea})(\text{Htea})_4]$  (2) with atom numbering scheme. Hydrogen atoms and disorder C and O atoms are omitted for clarity.

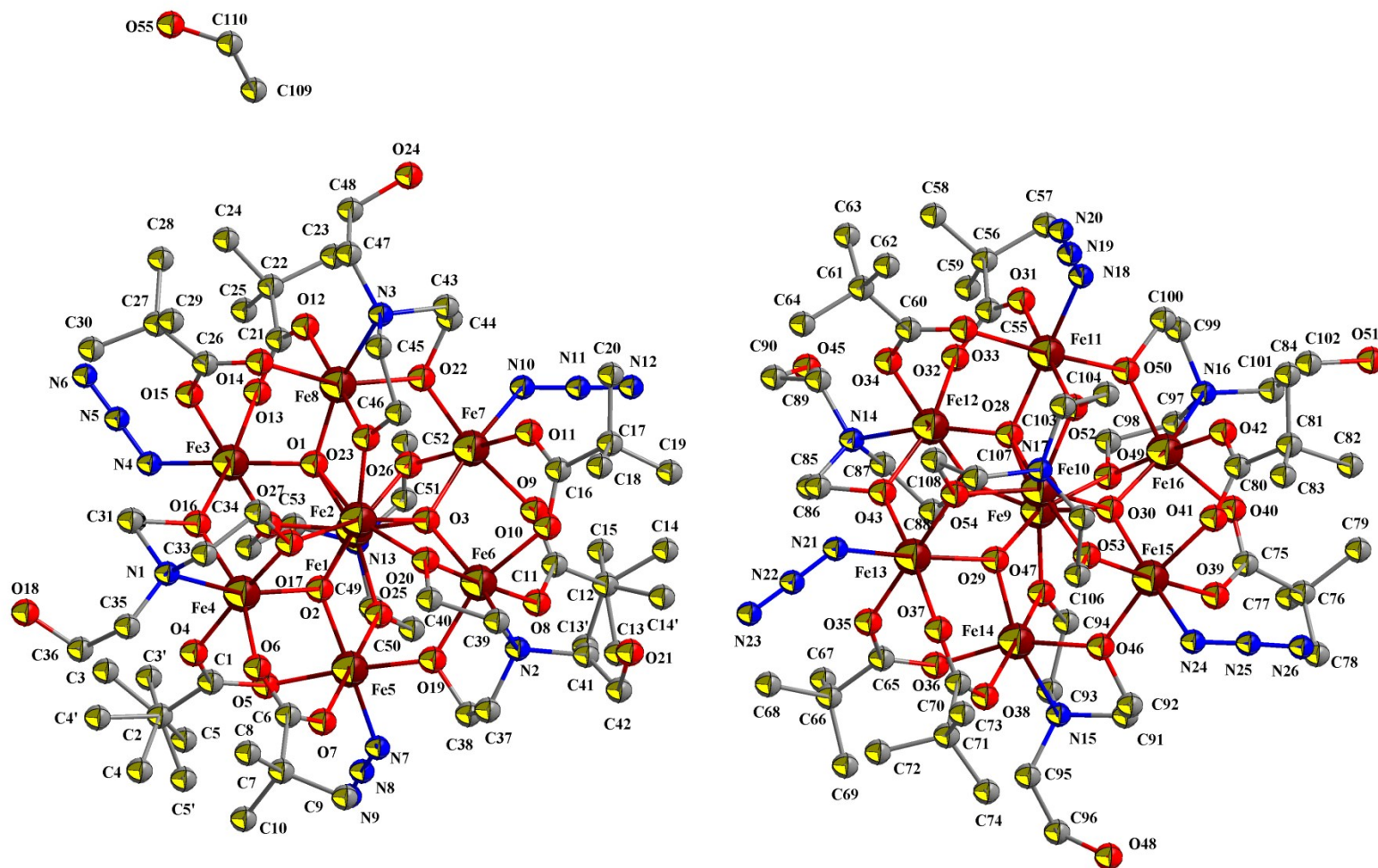


**Figure S4.** Asymmetric unit in the solid-state structure of  $[\text{Fe}_8\text{O}_2(\text{O}_2\text{CCMe}_3)_6(\text{N}_3)_3(\text{tea})(\text{Htea})_4] \cdot 0.5(\text{EtOH})$  (**3**) with atom numbering scheme. Hydrogen atoms are omitted for clarity.

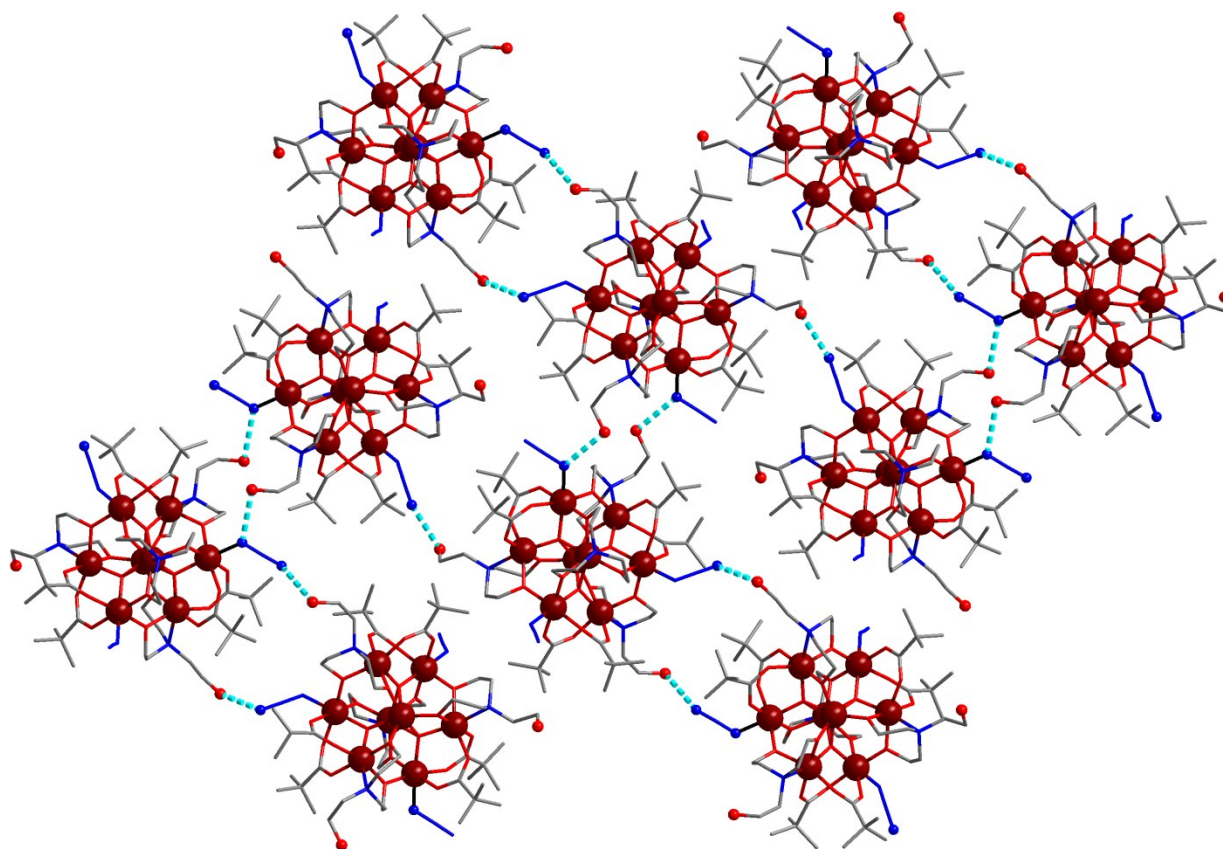


**Figure S5.** 2D layer formed in **3** through O–H···N interactions between protonated O atoms from  $\text{teaH}^{2-}$  and N atoms (azide). Intermolecular hydrogen bonds shown as dashed blue lines. All hydrogen atoms and solvent ethanol molecules are omitted for clarity. Color scheme: Fe, brown spheres; O, red; N, blue; C, grey sticks. Oxygen and nitrogen atoms that form hydrogen bonds are shown as red and blue balls, respectively.



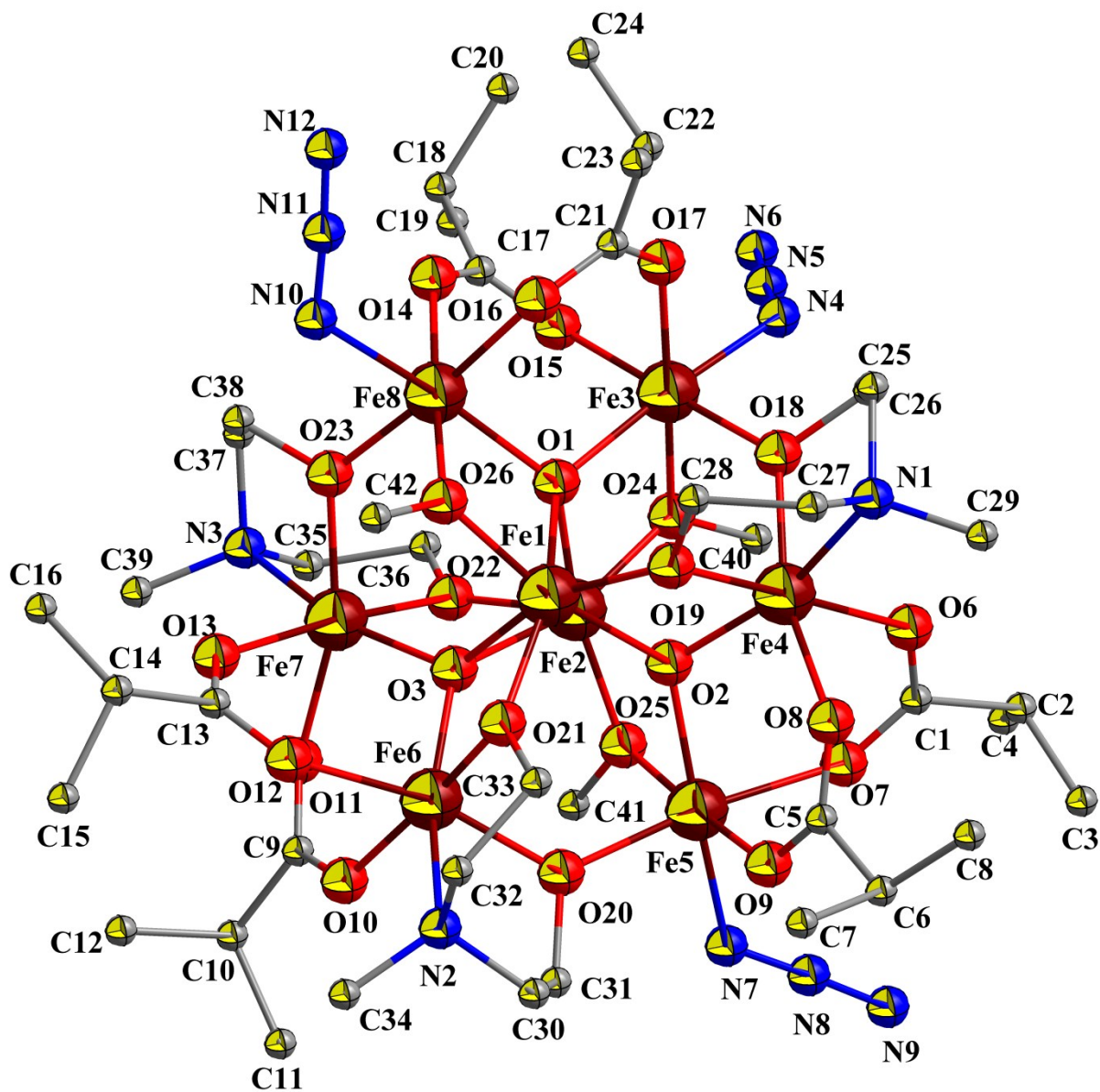


**Figure S6.** Asymmetric unit in the solid-state structure of  $[\text{Fe}_8\text{O}_3(\text{O}_2\text{CCHMe}_2)_6(\text{N}_3)_3(\text{mdea})_3(\text{MeO})_3]$  (**4**) with atom numbering scheme. Hydrogen atoms are omitted for clarity.

**Table S1.** BVS values<sup>a</sup>

[Fe <sub>8</sub> O <sub>3</sub> (O <sub>2</sub> CCHMe <sub>2</sub> ) <sub>9</sub> (tea) (teaH) <sub>3</sub> ]·MeCN·2(H <sub>2</sub> O) (1)				[Fe <sub>8</sub> O <sub>3</sub> (O <sub>2</sub> CCHMe <sub>2</sub> ) <sub>6</sub> (N <sub>3</sub> ) <sub>3</sub> (tea) (teaH) <sub>3</sub> ] (2)	
Fe1	3.188	Fe5	3.130	Fe1	2.816
Fe2	2.799	Fe6	3.007	Fe2	3.142
Fe3	3.197	Fe7	3.182	Fe3	2.985
Fe4	3.029	Fe8	3.031	Fe4	3.031
[Fe <sub>8</sub> O <sub>3</sub> (O <sub>2</sub> CCMe <sub>3</sub> ) <sub>6</sub> (N <sub>3</sub> ) <sub>3</sub> (tea)(teaH) <sub>3</sub> ]·0.5(EtOH) (3)				[Fe <sub>8</sub> O <sub>3</sub> (O <sub>2</sub> CCHMe <sub>2</sub> ) <sub>6</sub> (N <sub>3</sub> ) <sub>3</sub> (mdea) <sub>3</sub> (MeO) <sub>3</sub> ] (4)	
Fe1	2.711	Fe9	3.146	Fe1	3.153
Fe2	3.169	Fe10	2.770	Fe2	3.172
Fe3	3.112	Fe11	3.088	Fe3	3.130
Fe4	3.025	Fe12	3.035	Fe4	3.057
Fe5	3.130	Fe13	3.114	Fe5	3.066
Fe6	2.982	Fe14	3.026	Fe6	3.084
Fe7	3.088	Fe15	3.138	Fe7	3.074
Fe8	3.007	Fe16	2.955	Fe8	3.057

[a] N. E. Brese and M. O’Keeffe, *Acta Crystallogr.*, 1991, **B47**, 192; W. Liu and H.H. Thorn, *Inorg Chem.*, 1993, **32**, 4102.



### TGA/DTA data

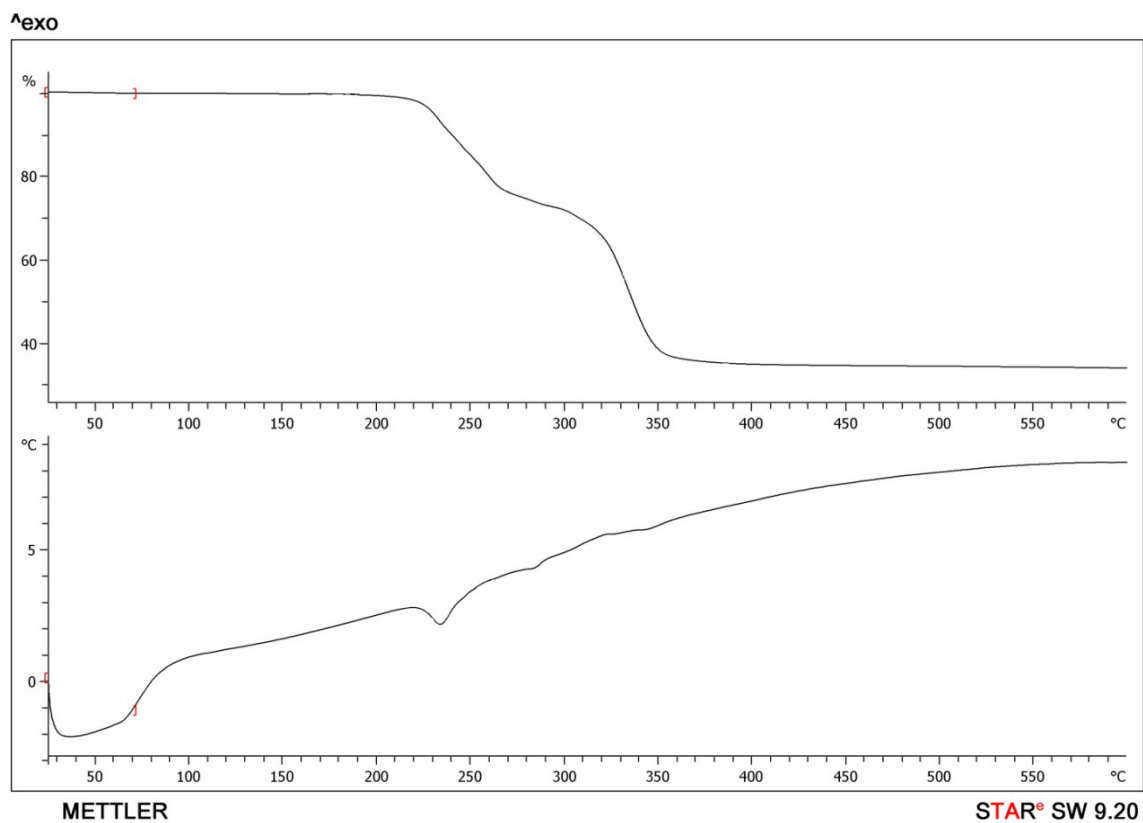


Figure S7. TGA/DTA curves of  $[\text{Fe}_8\text{O}_3(\text{O}_2\text{CCHMe}_2)_9(\text{tea})(\text{teaH})_3] \cdot \text{MeCN} \cdot 2(\text{H}_2\text{O})$  (1).

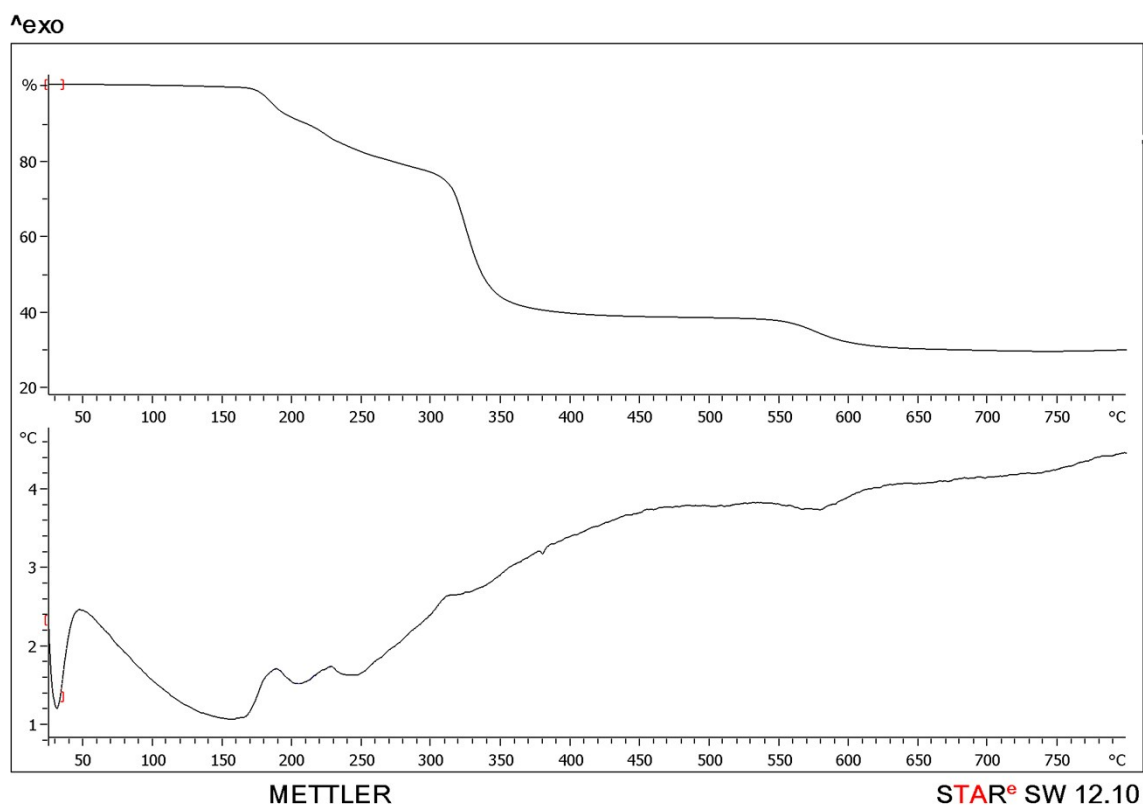
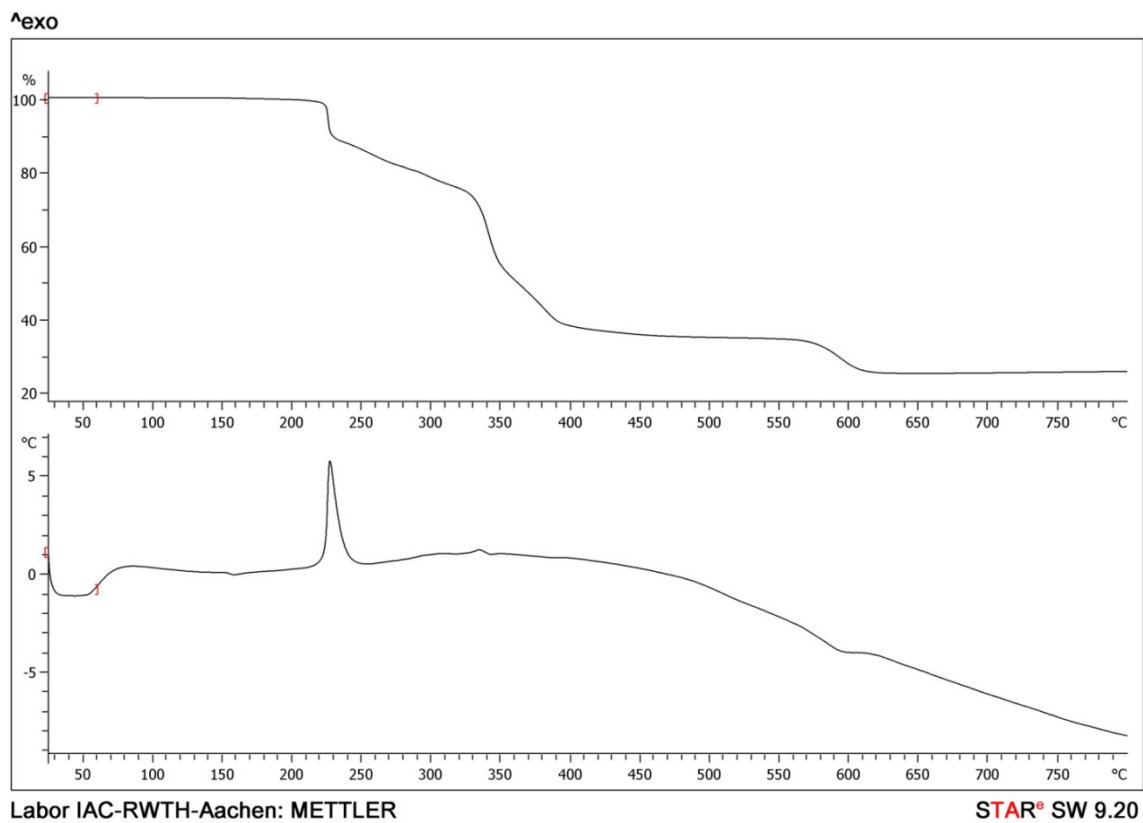
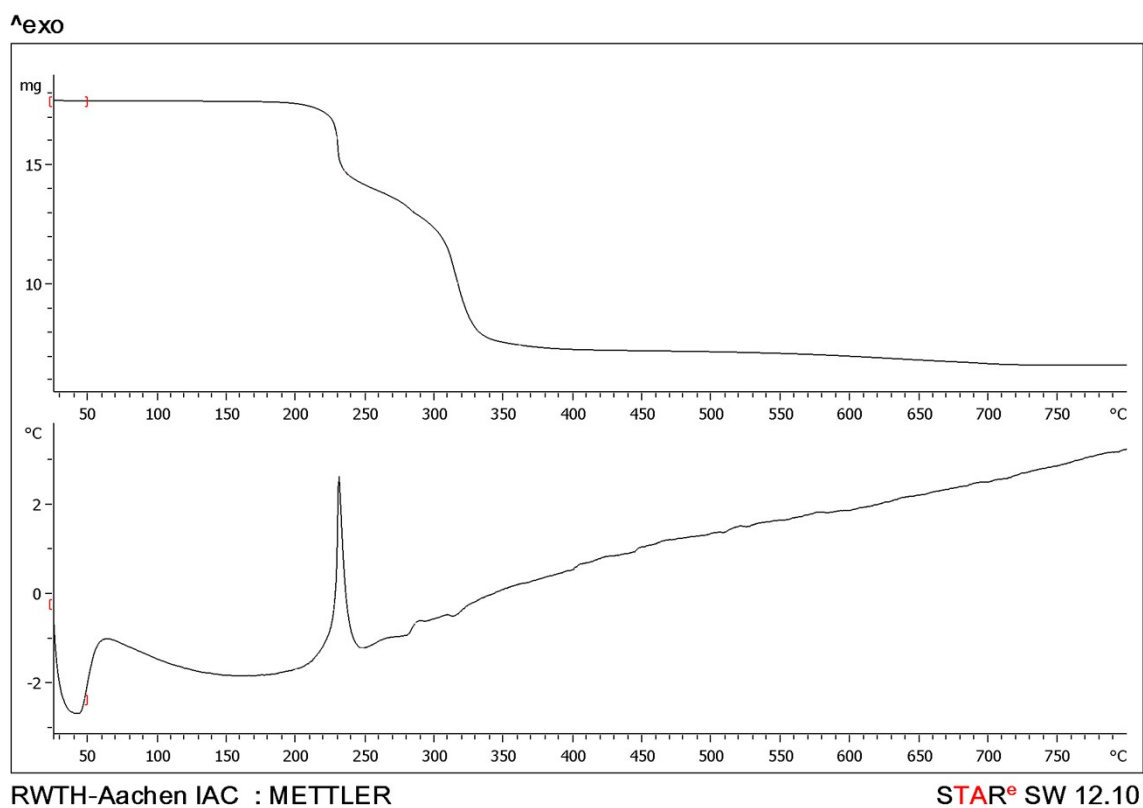


Figure S8. TGA/DTA curves of  $[\text{Fe}_8\text{O}_3(\text{O}_2\text{CCHMe}_2)_6(\text{N}_3)_3(\text{tea})(\text{teaH})_3]$  (2).



**Figure S9.** TGA/DTA curves for  $[\text{Fe}_8\text{O}_2(\text{O}_2\text{CCMe}_3)_6(\text{N}_3)_3(\text{tea})(\text{teaH})_4] \cdot 0.5(\text{EtOH})$  (**3**).



**Figure S10.** TGA/DTA curves for  $[\text{Fe}_8\text{O}_3(\text{O}_2\text{CCHMe}_2)_6(\text{N}_3)_3(\text{mdea})_3(\text{MeO})_3]$  (**4**).

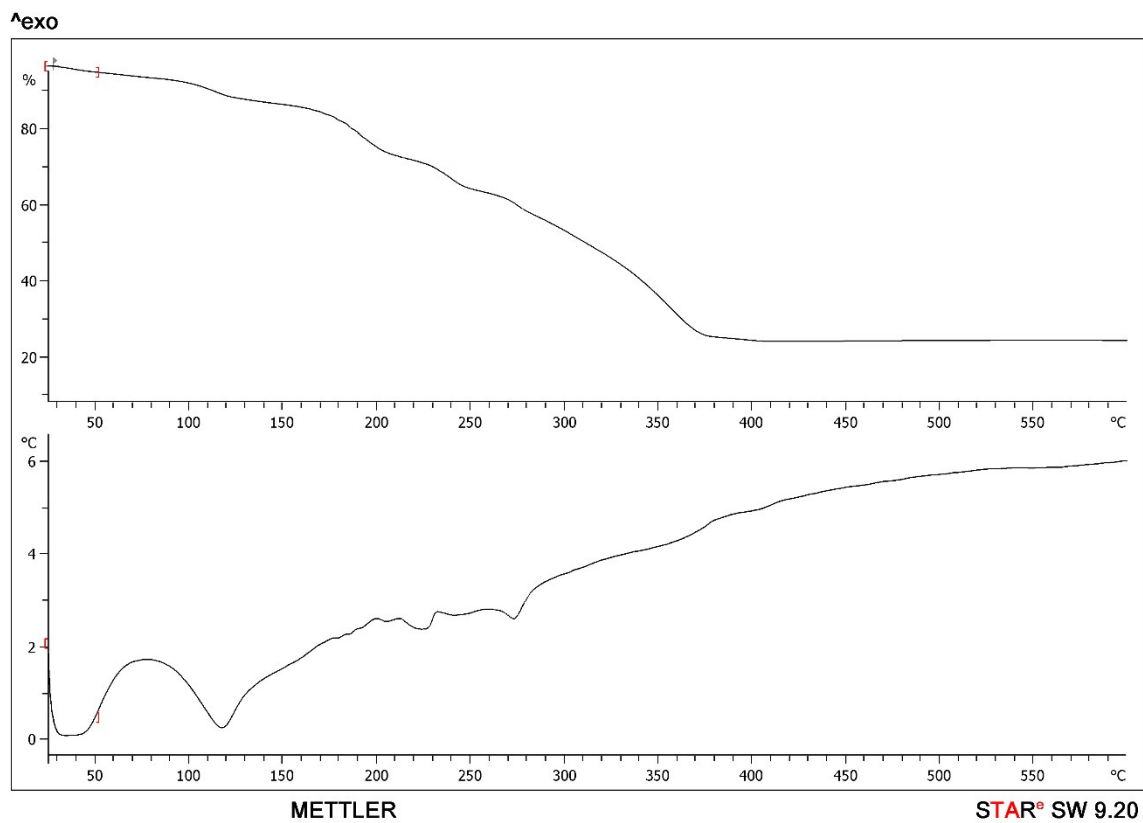


**Figure S11.** TGA/DTA curves of  $[\text{Fe}_3\text{O}(\text{O}_2\text{CCHMe}_2)_6(\text{H}_2\text{O})_3]\text{NO}_3 \cdot 2(\text{MeCN}) \cdot 2(\text{H}_2\text{O})$  (**5**).

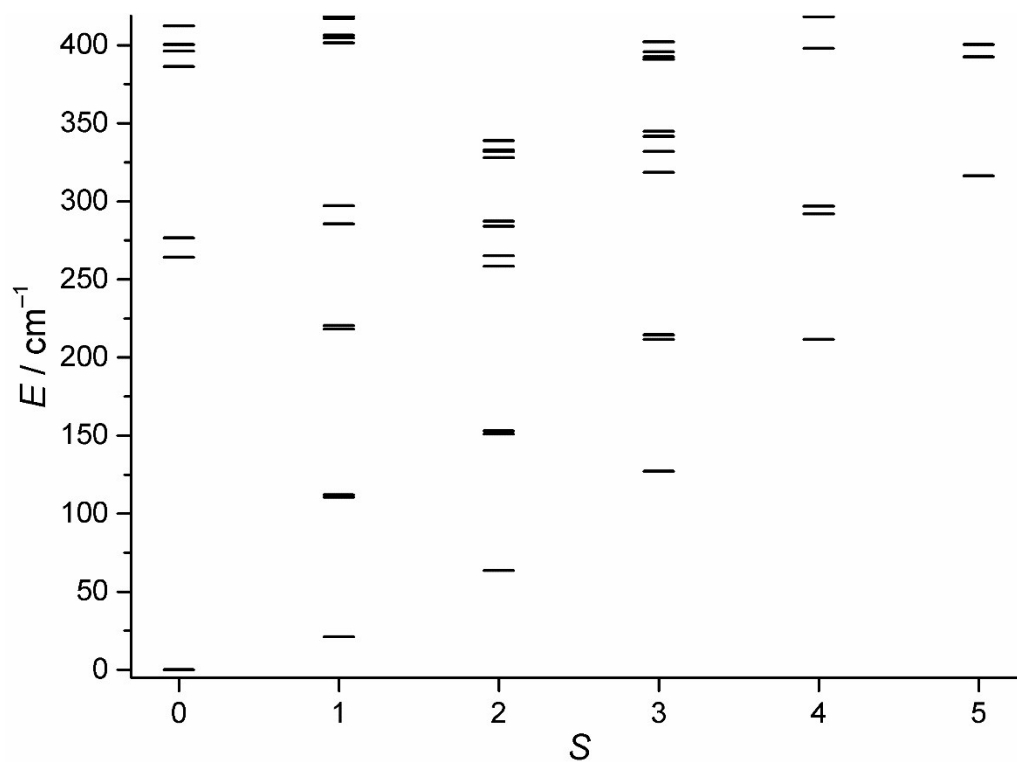


**Figure S12.** Calculated lowest energies  $E$  of total effective spin  $S$  states based on least-squares fit parameters for  $[\text{Fe}_8\text{O}_3(\text{O}_2\text{CCHMe}_2)_9(\text{tea})(\text{teaH})_3] \cdot \text{MeCN} \cdot 2(\text{H}_2\text{O})$  (**1**).

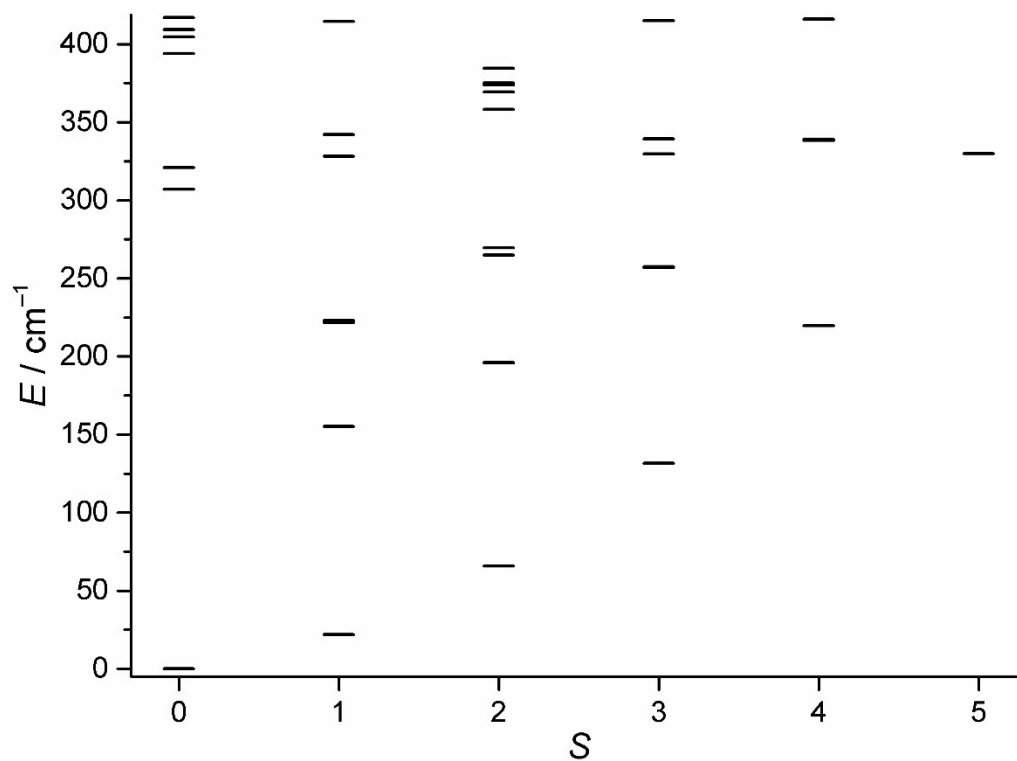


**Figure S13.** Calculated lowest energies  $E$  of total effective spin  $S$  states based on least-squares fit parameters for  $[\text{Fe}_8\text{O}_3(\text{O}_2\text{CCHMe}_2)_6(\text{N}_3)_3(\text{tea})(\text{teaH})_3]$  (**2**).

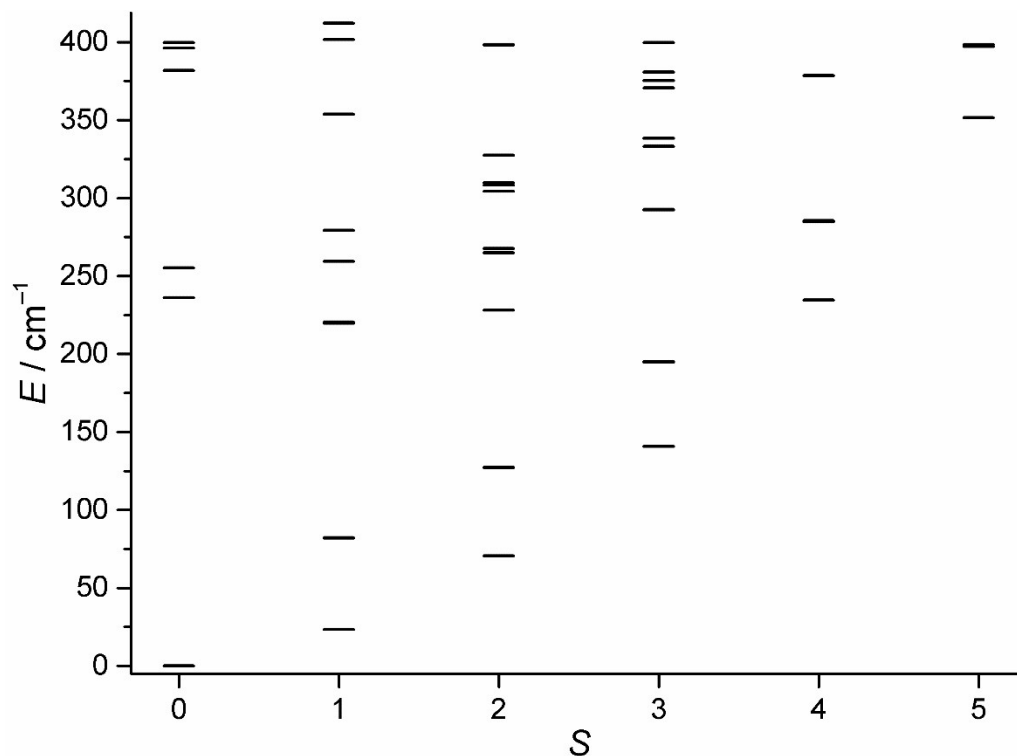


**Figure S14.** Calculated lowest energies  $E$  of total effective spin  $S$  states based on least-squares fit parameters for  $[\text{Fe}_8\text{O}_2(\text{O}_2\text{CCMe}_3)_6(\text{N}_3)_3(\text{tea})(\text{teaH})_4] \cdot 0.5(\text{EtOH})$  (3).

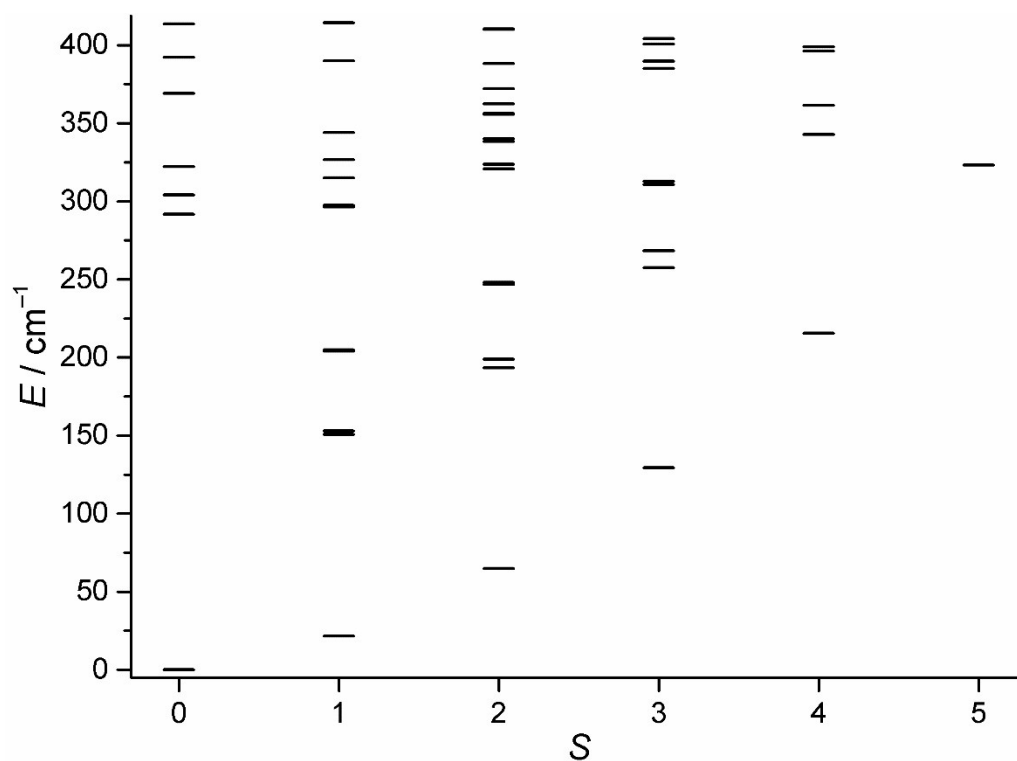


**Figure S15.** Calculated lowest energies  $E$  of total effective spin  $S$  states based on least-squares fit parameters for  $[\text{Fe}_8\text{O}_3(\text{O}_2\text{CCHMe}_2)_6(\text{N}_3)_3(\text{mdea})_3(\text{MeO})_3]$  (4).

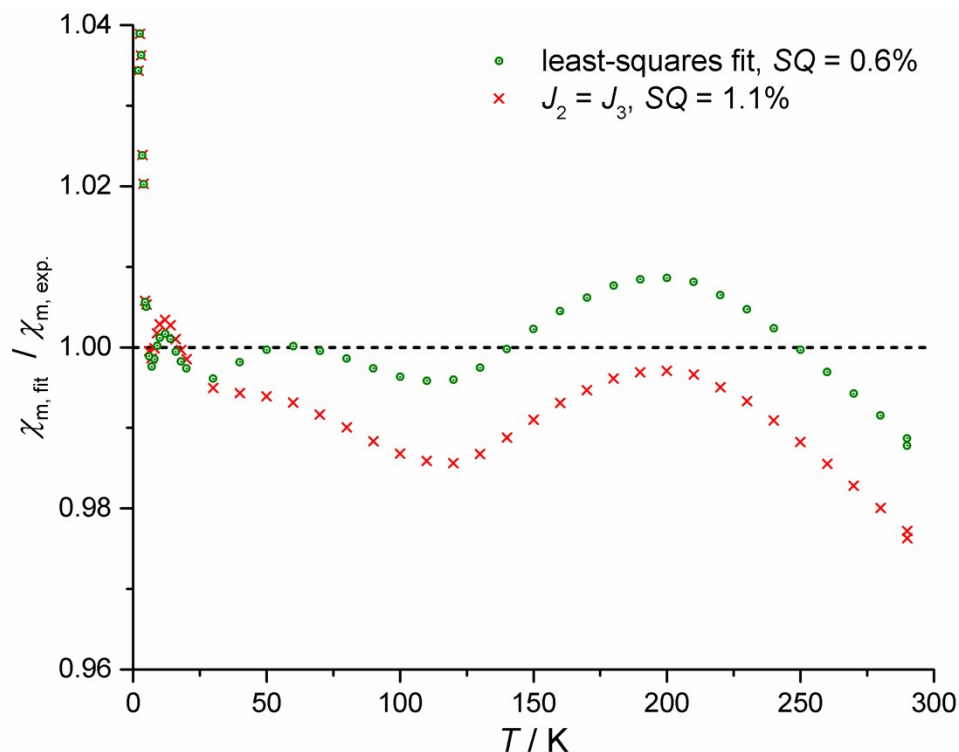


**Figure S16.** Comparison of the relative deviations of the 5- $J_i$  and 4- $J_i$  (setting  $J_3$  to the value of  $J_3$ ) model data from experimental  $\chi_m$  data for **1**. The dashed horizontal line at 1.00 represents the hypothetical situation of a perfect fit ( $\chi_{m,\text{fit}} \equiv \chi_{m,\text{exp.}}$ ).

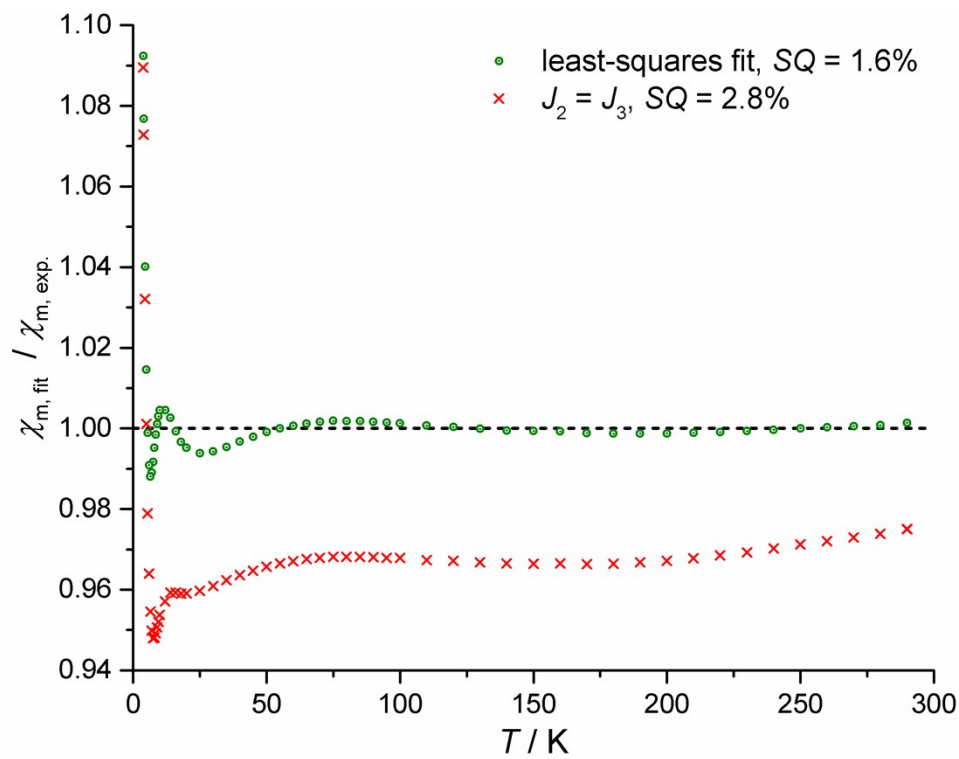


**Figure S17.** Comparison of the relative deviations of the 6- $J_i$  and 5- $J_i$  ( $J_2 = J_3$ ) model data from experimental  $\chi_m$  data for **4**. As in Fig. S16, a value of 1.00 would represent a perfect fit ( $\chi_{m,\text{fit}} \equiv \chi_{m,\text{exp.}}$ ).



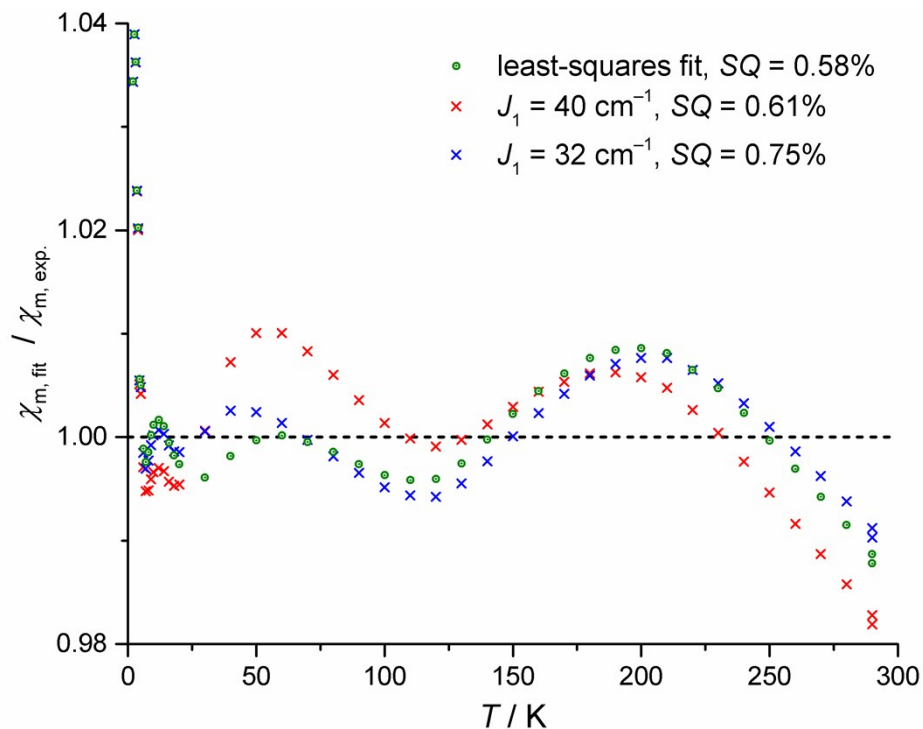


**Figure S18.** Influence of changes to  $J_1$ , the fitting parameter with the most correlation coefficients close to  $\pm 1$ . Shown are the relative deviations resulting from fixing  $J_1$  to values that have been arbitrarily modified ( $\pm 10\%$ ) compared to the least-squares fitting results. For the  $+10\%$  modification ( $J_1 = 40 \text{ cm}^{-1}$ ), the resulting least-squares fit yields  $J_2 = -23.0 \text{ cm}^{-1}$ ,  $J_3 = -22.7 \text{ cm}^{-1}$ ,  $J_4 = -14.9 \text{ cm}^{-1}$ ,  $J_5 = -9.1 \text{ cm}^{-1}$ . For the  $-10\%$  modification ( $J_1 = 32 \text{ cm}^{-1}$ ),  $J_2 = -26.6 \text{ cm}^{-1}$ ,  $J_3 = -19.3 \text{ cm}^{-1}$ ,  $J_4 = -11.6 \text{ cm}^{-1}$ ,  $J_5 = -11.3 \text{ cm}^{-1}$ .

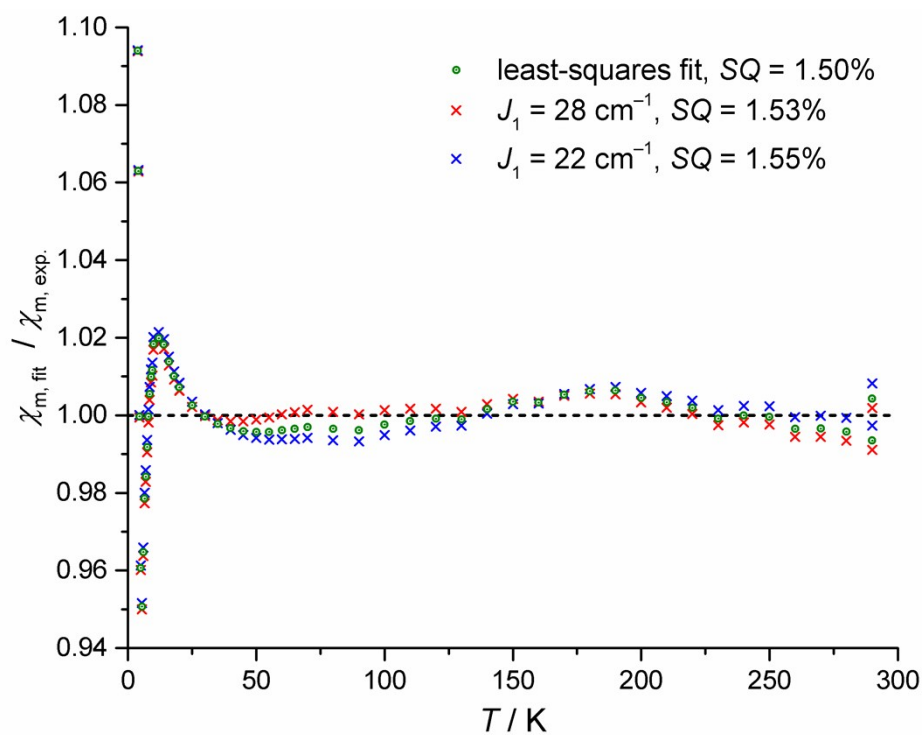


**Figure S19.** Same as Fig. S18, for compound **2**. Fixing  $J_1$  to 28 and 22  $\text{cm}^{-1}$ , the related fits yield  $J_2 = -22.9 \text{ cm}^{-1}$ ,  $J_3 = -21.9 \text{ cm}^{-1}$ ,  $J_4 = -12.5 \text{ cm}^{-1}$ ,  $J_5 = -10.6 \text{ cm}^{-1}$ , and  $J_2 = -22.2 \text{ cm}^{-1}$ ,  $J_3 = -20.6 \text{ cm}^{-1}$ ,  $J_4 = -18.4 \text{ cm}^{-1}$ ,  $J_5 = -3.7 \text{ cm}^{-1}$ , respectively.

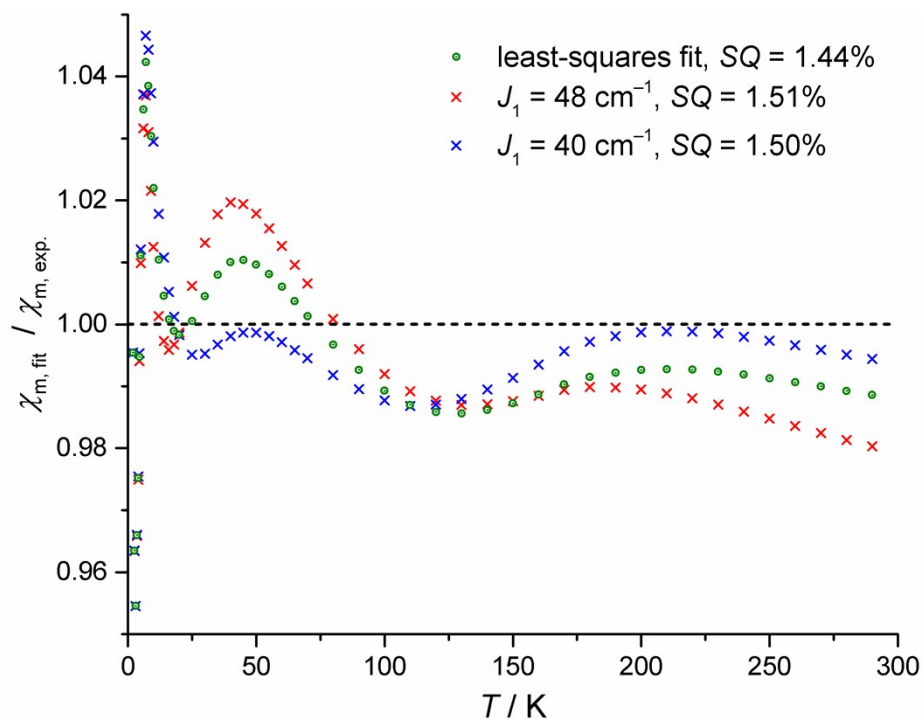


**Figure S20.** Same as Fig. S18, for compound **3**. Fixing  $J_1$  to 48 and 40  $\text{cm}^{-1}$ , the related fits yield  $J_2 = -22.7 \text{ cm}^{-1}$ ,  $J_3 = -22.7 \text{ cm}^{-1}$ ,  $J_4 = -19.9 \text{ cm}^{-1}$ ,  $J_5 = -7.0 \text{ cm}^{-1}$ , and  $J_2 = -22.1 \text{ cm}^{-1}$ ,  $J_3 = -22.1 \text{ cm}^{-1}$ ,  $J_4 = -20.0 \text{ cm}^{-1}$ ,  $J_5 = -5.8 \text{ cm}^{-1}$ , respectively.

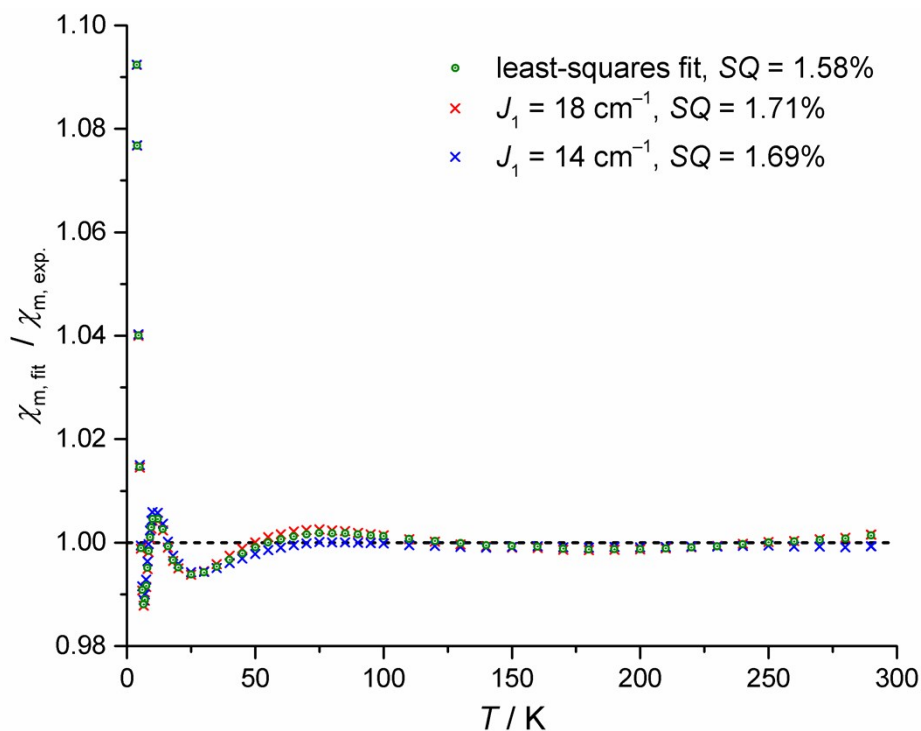


**Figure S21.** Same as Fig. S18, for compound **4**. Fixing  $J_1$  to 18 and 14  $\text{cm}^{-1}$ , the related fits yield  $J_2 = -17.5 \text{ cm}^{-1}$ ,  $J_3 = -17.2 \text{ cm}^{-1}$ ,  $J_4 = -10.3 \text{ cm}^{-1}$ ,  $J_5 = -36.2 \text{ cm}^{-1}$ ,  $J_6 = -14.0 \text{ cm}^{-1}$ , and  $J_2 = -17.3 \text{ cm}^{-1}$ ,  $J_3 = -17.0 \text{ cm}^{-1}$ ,  $J_4 = -9.6 \text{ cm}^{-1}$ ,  $J_5 = -46.2 \text{ cm}^{-1}$ ,  $J_6 = -12.0 \text{ cm}^{-1}$ , respectively.

### Correlation coefficients for magnetic exchange energies

The correlation coefficients<sup>[b]</sup> ( $\rho_{ik} = \text{cov}(J_i, J_k) / [\text{var}(J_i) \cdot \text{var}(J_k)]$ ) of the various least-squares fit parameters have been calculated (Tables S2–S5) to estimate their linear interdependencies. The interdependencies vary for each compound; however,  $J_1$  seems to generally feature the strongest correlation with the other parameters.

[b] Encyclopedia of Mathematics, Ed. M. Hazewinkel, Springer, London, 2010; Correlation coefficient. A.V. Prokhorov (originator), Encyclopedia of Mathematics, [http://www.encyclopediaofmath.org/index.php?title=Correlation\\_coefficient&oldid=12284](http://www.encyclopediaofmath.org/index.php?title=Correlation_coefficient&oldid=12284).

**Table S2.** Correlation coefficients of best fit for compound **1** ( $\rho_{ik} = \rho_{ki}$ ).

$\rho$	$J_1$	$J_2$	$J_3$	$J_4$	$J_5$
$J_1$	1	+0.811	+0.953	-0.726	-0.129
$J_2$	—	1	+0.926	-0.706	-0.634
$J_3$	—	—	1	+0.777	-0.418
$J_4$	—	—	—	1	+0.452
$J_5$	—	—	—	—	1

**Table S3.** Correlation coefficients of best fit for **2** ( $\rho_{ik} = \rho_{ki}$ ).

$\rho$	$J_1$	$J_2$	$J_3$	$J_4$	$J_5$
$J_1$	1	+0.984	+0.984	+0.019	-0.302
$J_2$	—	1	+0.932	+0.014	-0.303
$J_3$	—	—	1	+0.014	-0.303
$J_4$	—	—	—	1	+0.947
$J_5$	—	—	—	—	1

**Table S4.** Correlation coefficients of best fit for **3** ( $\rho_{ik} = \rho_{ki}$ ).

$\rho$	$J_1$	$J_2$	$J_3$	$J_4$	$J_5$
$J_1$	1	-0.715	+0.715	+0.623	-0.627
$J_2$	—	1	-0.984	-0.455	+0.555
$J_3$	—	—	1	+0.455	-0.555
$J_4$	—	—	—	1	-0.978
$J_5$	—	—	—	—	1

**Table S5.** Correlation coefficients of best fit for **4** ( $\rho_{ik} = \rho_{ki}$ ).

$\rho$	$J_1$	$J_2$	$J_3$	$J_4$	$J_5$	$J_6$
$J_1$	1	+0.056	+0.018	+0.030	+0.087	+0.724
$J_2$	—	1	+0.310	+0.452	-0.878	+0.369
$J_3$	—	—	1	+0.140	+0.530	+0.115
$J_4$	—	—	—	1	-0.511	+0.167
$J_5$	—	—	—	—	1	+0.108
$J_6$	—	—	—	—	—	1